EurJOC European Journal of Organic Chemistry

FULL PAPER

DOI: 10.1002/ejoc.201301218

The Remarkable Hyperchromicity of Ketohydrazone Dyes and Pigment Lakes Derived from 4-Morpholino-2-naphthol

Stuart Aiken,[a] Christopher D. Gabbutt,[a] Lisa J. Gillie,[a] Jonathan D. Heywood,[a] Denis Jacquemin,[b,c] Craig R. Rice,[a] and B. Mark Heron*[a]

Keywords: Ketohydrazones / Dyes/pigments / Density functional calculations / Structure elucidation / Synthesis design

The syntheses of a series of new ketohydrazone dyes and pigment lakes with a unique structural motif derived from 4-morpholino-2-naphthol are described. The morpholine substituent is responsible for the hypsochromically shifted absorption maxima with significantly enhanced molar extinction coefficients of the new dyes; this conclusion is supported by time-dependent DFT (TD-DFT) simulations. The location of the morpholine substituent at a sterically demanding site in the pigment lake obstructs further coordination of the bridging sulfonate groups in the solid state and prevents the formation of a 1-dimensional polymeric system, which is common for other pigment lakes.

Introduction

The study of dyes and pigments has been of immense societal impact since antiquity. Today, our daily interactions with colourants include traditional textile and polymer coloration for aesthetic purposes, dyes in recording media such as compact discs (CDs) and Blu-ray Discs™, traditional writing inks to new ink-jet and laser printing systems, as well as dyes in medicine from the original antibacterial azo dye Prontosil through to modern antibacterial and antitumour dye sensitizers in photodynamic therapy. Dye chemistry research is presently thriving with the design of numerous sensors and functional dyes and, perhaps more importantly, the evolution of dyes in the energy arena such as low power-consumption light-emitting diodes and dyes optimized for efficient solar-energy conversion in dye-sensitized solar cells. Finally, the economic impact of the industrial manufacture and application of coulorants makes a significant contribution to the gross domestic product (GDP) of numerous countries, a feature that ensures constant activity in colourant research.

[a] Department of Chemical and Biological Sciences, The University of Huddersfield,
Queensgate, Huddersfield, HD1 3DH, UK
E-mail: m.heron@hud.ac.uk
http://www.hud.ac.uk/
[b] CEISAM, UMR CNRS 6230, Chimie et Interdisciplinarité, Synthèse, Analyse, Modélisation, Université de Nantes, Faculté des Sciences et des Techniques,
BP 92208, 2 rue de la Houssinière, 44322 Nantes Cedex 3 France
[c] Insitut Universitaire de France (IUF),
103 Blvd Saint Michel, 75005 Paris Cedex 5 France
Supporting information for this article is available on the WWW under http://dx.doi.org/10.1002/ejoc.201301218.

4-Morpholino-2-naphthol (**1**) has been a privileged building block for the synthesis of commercially successful photochromic naphthopyrans for two decades.[1–5] The synthesis of **1** was first described by Gabbutt et al. and involved the dichlorination of 2-naphthol to afford 1,1-dichloronaphthalenone (**2**), the in situ nucleophilic addition of morpholine and concomitant elimination of a chloride ion to afford **3** and subsequent removal of the remaining chlorine atom by catalytic hydrogenation (Scheme 1).[1] The foregoing procedure is an adaptation of a route employed to access 4-methoxy-2-naphthol by the addition of methoxide to **2** reported in 1970.[6] The nucleophilic displacement of the 1-chloro substituent of intermediate **3** by amines and thiols has been investigated.[7] An alternative route to **1** has been reported and includes the preparation of a mixture of hydrazones **4a** and **4b** followed by alkaline hydrolysis with Wolff–Kishner-like decomposition.[2] More recently, a selection of 4-amino-2-naphthols has been accessed by the transition-metal-mediated amination of 3-methoxy-1-(trifluoromethylsulfonyloxy)naphthalene with a variety of amines and subsequent demethylation.[8]

2-Naphthol and numerous substituted derivatives have been widely employed in the colourant industry as coupling components with an extensive array of diazonium salts to afford commercially significant dyes and pigments.[9,10] It is remarkable that the application of **1** in this respect has been overlooked. Here, we report preliminary results on the investigation of the synthesis and spectroscopic properties of hitherto unexplored ketohydrazone (azoenol) dyes and pigment lakes derived from 4-morpholino-2-naphthol.

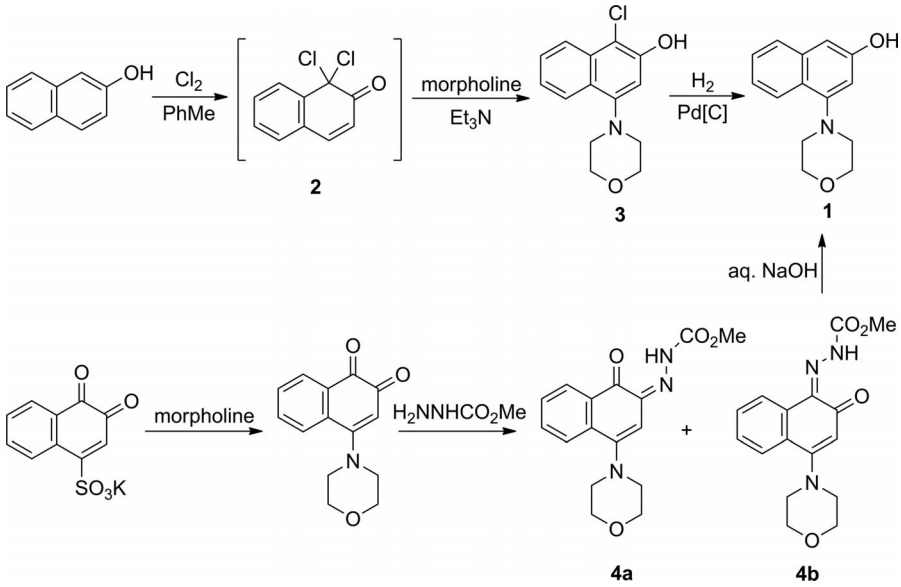

Scheme 1. Synthesis of 4-morpholino-2-naphthol.

Results and Discussion

A series of anilines **5** (**a**: R = H; **b**: R = Me; **c**: R = MeO; **d**: R = Cl) were diazotized and coupled to a suspension of **1** in sodium hydroxide by using standard diazotization and coupling methodology.[9–11] A slight change to the standard diazotization protocol was adopted for 4-nitroaniline (**5e**):[9–11] A fine suspension of the aniline hydrochloride was employed for the diazotization reaction rather than a solution of the aniline hydrochloride as for **5a**–**d**. The crude dyes **6a**–**e** were isolated, washed well with water and dried before crystallization from a minimum volume of acetic acid to afford the pure dyes in 56–69% yield as bright orange solids (Scheme 2). The diazotization of orthanilic acid (2-aminobenzenesulfonic acid)[9–11] and coupling to **1** to afford dye **8** in 84% yield was also examined (Scheme 3). For comparative purposes, dyes **9a** (Sudan I) and **10**

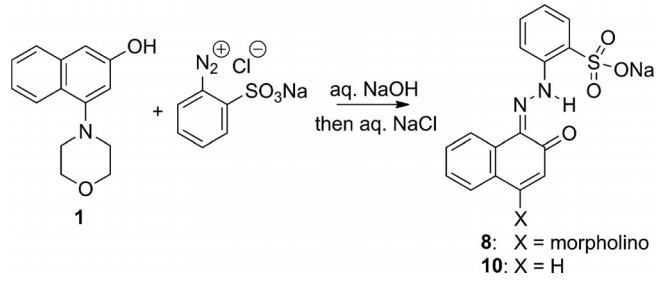

Scheme 3. Preparation of dyes **8** and **10** derived from orthanilic acid.

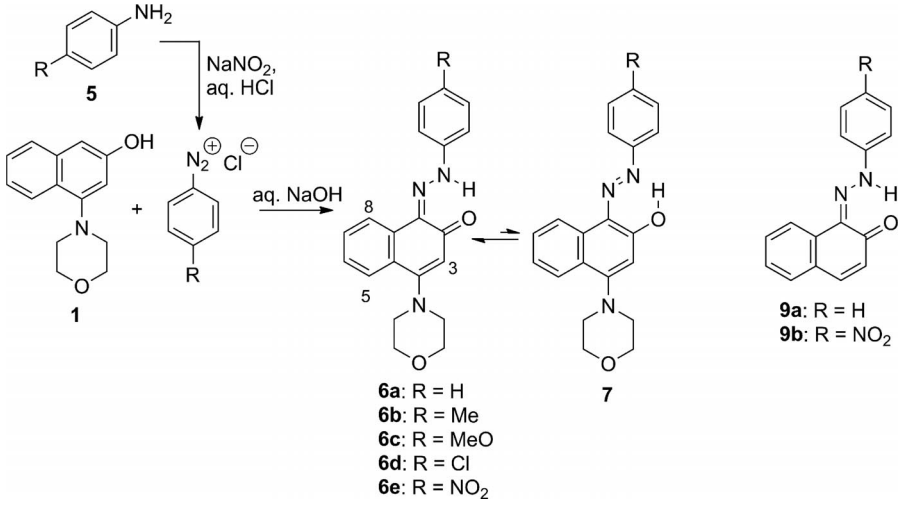

Scheme 2. Preparation of dyes **6a**–**e**.

derived from 2-naphthol and aniline in 71% yield and from 2-naphthol and orthanilic acid in 75% yield, respectively, were also prepared.

The examination of **6** in $CDCl_3$ solution by NMR spectroscopy revealed that 5-H and 8-H typically appeared as a double doublet at $\delta \approx 7.7$ and 8.5 ppm, respectively, whereas 3-H appeared as a singlet at $\delta \approx 6.1$–6.4 ppm. The signal for 3-H in **9a** appeared as a doublet at $\delta = 6.89$ ppm with $J = 9.4$ Hz, which reflects *cis*-alkene-like coupling to 4-H.[12] A low-field exchangeable signal was apparent at $\delta \approx 16.0$–16.4 ppm, which we have arbitrarily assigned (vide infra) to the H-bonded NH group of the major hydrazone tautomer **6** rather than the OH group of the azo tautomer **7**. The presence of the morpholine group was established by signals at $\delta \approx 3.3$ and 4.0 ppm for the NCH_2 and OCH_2 units, respectively.

There has been a significant body of work published on azoenol/ketohydrazone tautomerism with data from X-ray crystallography,[13–15] solution[15,16] and solid-state ^{13}C NMR spectroscopy,[17] molecular modelling[18] and multinuclear NMR spectroscopy[12,19] employed to assign the major tautomeric form, which is of course dependent upon both substitution pattern and environment. In the absence of suitable crystals of **6** for X-ray crystallography coupled with its generally low solubility, which precluded natural-abundance ^{15}N NMR spectroscopy, we have commented upon the azo/hydrazone tautomerism in **6** by comparing published ^{13}C NMR spectroscopic data for azo dyes derived from 2-naphthols[12,15,16] with the data recorded for **6a**–**6e**.

^{13}C NMR spectroscopy for $CDCl_3$ solutions of **6a**–**e** revealed low-field signals in the range $\delta = 174$–181 ppm, assigned to a C=O function, together with a signal at $\delta \approx 161$ ppm for the hydrazone C=N group (Table 1). With simple azo dyes derived from 2-naphthol and 4-substituted anilines, the chemical shift of the C-2 signal has been used as a probe to gauge the ratio of the ketohydrazone/azoenol tautomers; when the phenyl group contains a strong electron-withdrawing group at the *para* position, the equilibrium shifts almost completely to the ketohydrazone tautomer as indicated by $\delta_{C\text{-}2} = 180$ ppm, and for an alkoxy-releasing group at the *para* position, $\delta_{C\text{-}2} \approx 161$ ppm.[15,16] In this work, although the magnitude of the chemical shifts are somewhat different, presumably as a consequence of conjugation with the morpholine unit at C-4, the trend in chemical shift (decreasing chemical shift of the C-2 signal with increasing donor group strength) is apparent, and it would be prudent to accept that, in common with the simple dyes derived from 2-naphthol, the dominant tautomer is the ketohydrazone but appreciate that in solution and in the solid state a hybrid of the two forms is the reality (Figure 1). Infrared spectroscopy revealed the presence of an intense C=O stretching band at ca. 1590–1606 cm^{-1} for **6**, the band for **6a** appeared at 1595 cm^{-1}, and the C=O stretching band for **9a** appeared at 1616 cm^{-1}; a comparison of the data for **6a** with that of **9a** indicates that the morpholine unit does have a marked influence on the CO bond order.

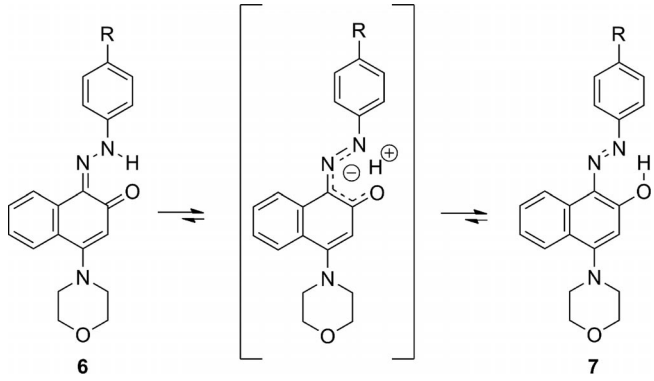

Figure 1. Ketohydrazone **6** and azoenol tautomer **7**.

Table 1. Selected ^{13}C NMR chemical shifts for **6** and **9a**.

Compound	R	$\delta_{C\text{-}2}$ [ppm]	$\delta_{C\text{-}1}$ [ppm]
9a	–	172.1	144.7
6a	H	178.7	161.2
6b	Me	177.8	160.7
6c	MeO	174.5	159.9
6d	Cl	178.8	161.4
6e	NO_2	180.9	162.7

The ^1H NMR spectrum of **8** in D_2O/[D_6]dimethyl sulfoxide ([D_6]DMSO) solution was recorded at low concentration as a consequence of its poor solubility in [D_6]DMSO alone; meaningful ^{13}C NMR data could not be obtained. The morpholine OCH_2 group resonated at $\delta = 3.78$ ppm, the signal of the NCH_2 group was observed at $\delta = 3.17$ ppm, and the signal of 3-H appeared as a singlet at $\delta = 5.96$ ppm. In contrast, the ^1H NMR spectrum of **10** revealed a doublet at $\delta = 6.63$ ppm with $J = 9.5$ Hz for 3-H. The infrared stretching band for the C=O function appeared at 1573 cm^{-1} for **8** and 1614 cm^{-1} for **10**. Thermogravimetric analysis of **8** and **10**, after the samples had been dried at 120 °C, revealed no evidence of hydrates on heating over the range 25–450 °C. However, decomposition to a black glass was noted at 340 and 310 °C for **8** and **10**, respectively; this suggests that the morpholine group enhances thermal stability.

The low solubility of **8** prompted us to examine its properties as a calcium lake pigment. Pigment lakes are typically alkaline earth metal salts of azo dyes containing either sulfonate or carboxylate groups and are widely used commodity colourants, which are typically employed for the colouration of paints and polymers and the production of high-volume printing inks.[10,20] There are several examples of pigment lakes derived from either 2-naphthol or 3-hydroxynaphthalene-2-carboxylic acid, especially when coupled with orthanilic acid derivatives, including **11** (a dichloro analogue of Ca4B toner), **12** (Lithol red, Pigment Red 49), **13** (Pigment Red 57:1) and **14** (Pigment Red 53:2; Figure 2). There has been recent interest in establishing the structure of pigment lakes by X-ray diffraction techniques, for example, the structures of **11**[21] and **12**[22] have been

determined by single-crystal X-ray diffraction, that of **13** by powder X-ray diffraction[23] and that of **14** by electron diffraction.[24]

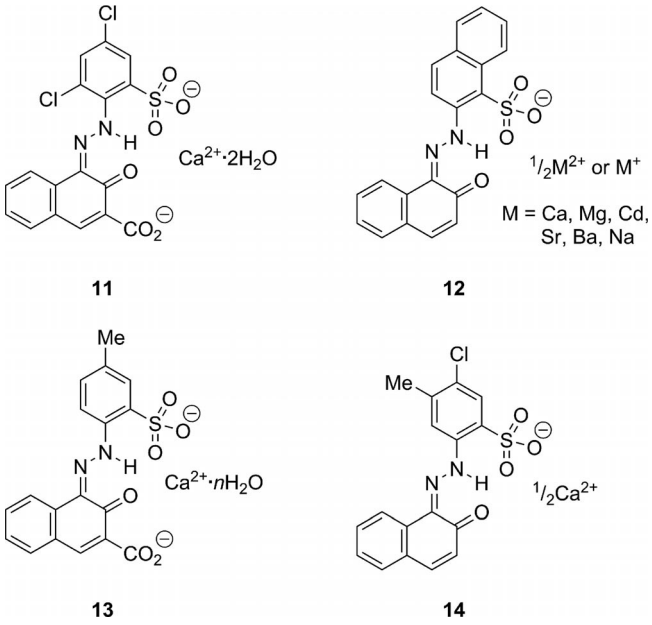

Figure 2. Examples of pigment lakes with known crystal structures.

A hot aqueous solution of $CaCl_2$ was added in a single portion to a vigorously stirred solution of **8** in hot water at ca. 80 °C, which resulted in the instantaneous production of an orange precipitate. The hot solution was stirred for a further 2 h and then cooled to ca. 40 °C, whereupon the crude lake **15** was collected by vacuum filtration, washed well with water and then dried (Scheme 4). It is fairly common practice in the preparation of pigments to use either a thermal treatment or solvent conditioning step, which may or may not be incorporated into the initial synthesis step.[10,25] In this instance, crude **15** was "conditioned" in two ways: (1) A sample of **15** was dissolved in a minimum of hot DMSO and allowed to crystallize as the solution gradually cooled to room temp., whereupon the product **15a** as fine red-orange microcrystals was collected by filtration and washed with Et_2O. (2) A sample of **15** was dissolved in a slight excess of hot DMSO, the solution was cooled to room temp. and then diluted with water, and the resulting precipitated orange solid **15b** was collected by filtration. Each sample was then dried in an oven at 120 °C. A similar protocol was employed for the preparation of **16** from **10** with conditioning as for **15b** followed by crystallization from aqueous DMSO.

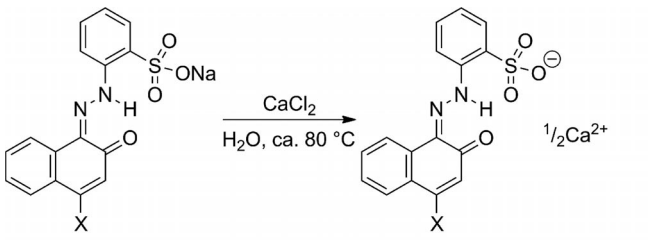

8: X = morpholino
10: X = H

15a: X = morpholino, from DMSO
15b: X = morpholino, from aq. DMSO
15c: X = morpholino, from heating of **15a**
16: X = H, from aq. DMSO

Scheme 4. Preparation of pigment lakes **15** and **16**.

An examination of the ^1H NMR spectrum of **15a** in [D_6]-DMSO revealed the expected signal at δ = 6.05 ppm for 3-H and a low-field signal at δ = 15.7 ppm attributed to the NH group together with a signal at δ = 2.54 ppm (s, 6 H). The latter signal, shifted marginally downfield of the residual [D_5]DMSO solvent signal (δ = 2.50 ppm), is attributed to solvated DMSO displaced upon dissolution of the complex. A corresponding signal for DMSO was evident in the ^{13}C NMR spectrum at δ = 40.9 ppm. In contrast, the ^1H and ^{13}C NMR spectra of **15b** exhibited no such DMSO signal, though the remaining ^1H and ^{13}C NMR signals had nearly identical chemical shifts to those of **15a**.

Noticeable differences in the thermogravimetric analyses of **15a** and **15b** were observed. A mass loss for **15a** commenced at ca. 200 °C and accounted for 1.7–1.9 equiv. DMSO; this suggests that **15a** is a bis(DMSO) solvate, which is corroborated by the foregoing NMR spectroscopic data. The formation of hydrates (and solvates) is common for various classes of lake pigments.[22,23,26] Further heating of **15a** revealed decomposition commencing at ca. 320 °C, and examination of the sample of **15a** after completion of the temperature cycle up to 450 °C revealed a black powder. By comparison, the thermogram of **15b** revealed a minor mass loss (ca. 2%) over the range 25–60 °C, which we have assigned to the loss of water, probably adsorbed from the atmosphere by the sample upon storage. There are no other mass events until the temperature approaches ca. 335 °C, whereupon decomposition is observed. This thermal profile suggests that either **15b** was isolated as a monohydrate (monohydrate requires 2.5% mass loss) that rapidly dehydrates at room temperature or as an anhydrate; the absence of any ligated DMSO was supported by NMR studies. To date, there has been only one other report of an anhydrate pigment lake derived from 2-naphthol, Pigment Red 53:2.[24] Thermal analysis of the model lake **16** revealed decomposition at ca. 330 °C.

As **15a** eliminated DMSO on thermal analysis, a sample was gradually warmed to 200 °C in a Büchi drying pistol under vacuum (5 mbar). The sample gradually darkened during this period to afford a red solid **15c**; examination of this sample in [D_6]DMSO by ^1H NMR spectroscopy revealed a spectrum that was essentially identical to that of **15a** but with the notable absence of any signals for DMSO.

An examination of the powder X-ray diffraction (PXRD) patterns of **15a** and **15b** (Figure 3) provided two key pieces of information. Firstly, the appearance of the pattern for **15a**, which had been isolated from DMSO, indicated improved crystallinity over the pattern obtained for **15b**, which was isolated from aqueous DMSO. Secondly, allowing for the difference in their crystallinity, the two samples have quite different crystal structures, as evidenced by their different peak patterns, which confirm a different symmetry and unit-cell size. A simulated PXRD pattern, calculated by using Mercury[27] from the single-crystal data for **15a**,

confirmed that the polycrystalline powder sample exhibits the same crystal structure as the single-crystal sample and is indeed a single phase. The PXRD pattern for **15c** was markedly different from that of its precursor **15a** and exhibited poorly resolved and significantly broadened peaks (humps), which were indicative of a thermal transformation leading to an amorphous solid.

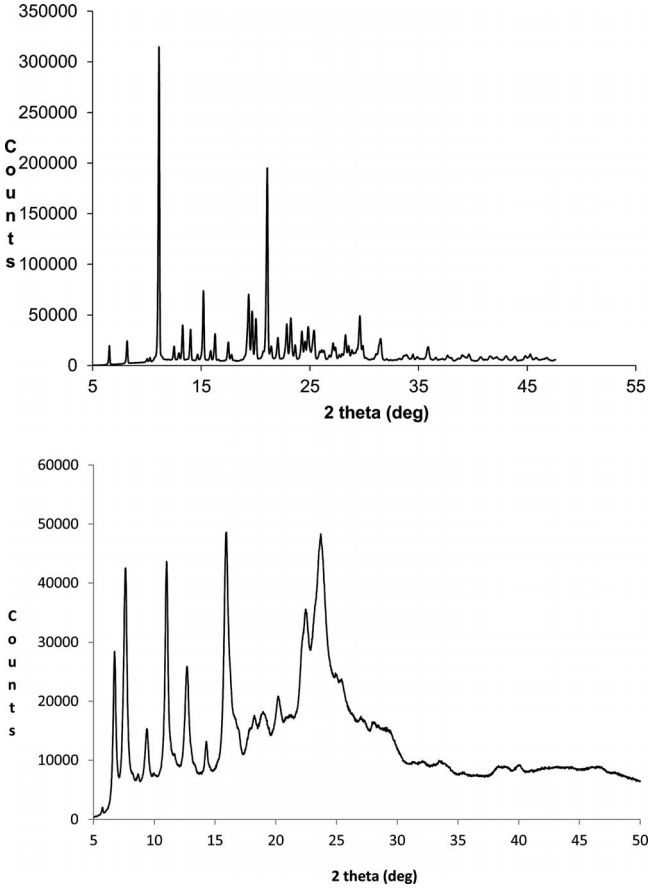

Figure 3. Powder X-ray diffractograms of **15a** (top) and **15b** (bottom).

Scanning electron micrographs (Figure 4) confirmed the microcrystalline nature of **15a** with the presence of aggregated rectangular crystals of varying dimensions up to ca. $24 \times 16 \times 9$ μm for the largest crystals. Although this size range falls outside the widely accepted crystal length of 0.1–0.5 μm at which pigments show their optimum colour/size dependence,[10,28] further solvent conditioning/crystallization offers potential improvement to the crystal dimensions.

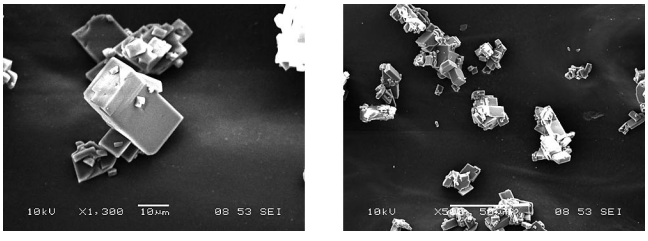

Figure 4. Scanning electron micrographs of **15a**.

Conscious of the fact that there are very few single-crystal X-ray structure determinations for 2-naphthol-derived pigment lakes[21,22] and acknowledging the difficulty other groups have experienced in obtaining suitable crystals for such single-crystal diffraction studies (e.g., small crystals requiring either synchrotron sources,[22] powder diffraction techniques,[23] or electron diffraction),[24] we were encouraged by the ease with which microcrystals of **15a** were obtained from DMSO. Thus, crystallization of **15a** was explored, and, gratifyingly, deep red-orange crystals suitable for X-ray diffraction were obtained from a DMSO solution after three weeks at room temperature and enabled the crystal structure of **15a** to be determined (Figures 5 and 6).[29]

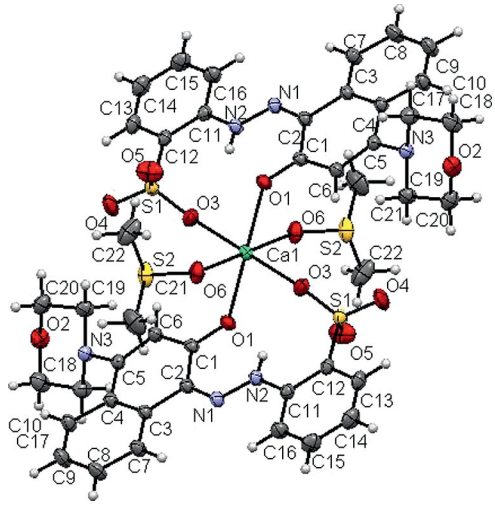

Figure 5. Single-crystal X-ray structure of **15a** as a displacement ellipsoid plot.

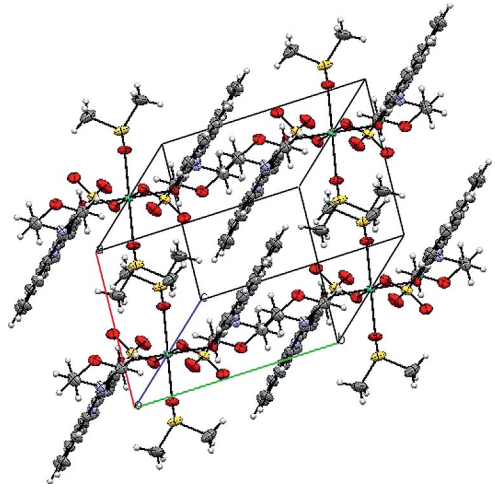

Figure 6. Crystal packing diagram for **15a**.

In the crystal structure of **15a**, the central calcium ion adopts a nearly octahedral geometry with the metal ion coordinated in the equatorial position by the oxygen atoms from the sulfonate and carbonyl groups from each ligand. The oxygen atoms of two *trans*-disposed molecules of DMSO complete the coordination sphere. The latter feature complements the observation of DMSO solvation from the

thermogravimetric and NMR analyses. The Ca–O bond lengths are 2.3151(8) (Ca–O6), 2.3183(7) (Ca–O1) and 2.3303(8) Å (Ca–O3); these bonds are marginally longer than those described for an anhydrate phase of Pigment Red 53:2 (**14**), for which the Ca–O bond lengths varied between 2.23 and 2.27 Å.[24] The O–Ca–O bond angles vary from ca. 85 to 95° and suggest a slightly distorted octahedron. The N–N bond of 1.3110(11) Å is longer than those (ca. 1.256–1.266 Å) reported for a series of nonphenolic sulfonated azo dyes, which have no opportunity to exhibit azoenol/ketohydrazone tautomerism,[30] and is marginally longer than those of several azo dyes derived from 2-naphthols, which appear in the range 1.277–1.308 Å.[14,15,31] A comparison of selected bond lengths for the azoenol/ketohydrazone unit of Ca^{2+} lake pigments **11** and **14** with those of **15a** confirmed observations that the organic ligand favours the ketohydrazone tautomer (Table 2).[21,23]

Table 2. Selected bond lengths for pigment lakes **15a**, **11**, and **14**.

Compound	Bond length [Å]		
	N–N	C–N	C–O
15a	1.311	1.327	1.270
11 from ref.[21]	1.304	1.333	1.257
14 from ref.[24]	1.29	1.35	1.31

For the most part, the structure is similar to that of the other reported pigment lakes in that the dye acts as a bidentate ligand and coordinates to the calcium ion through sulfonate and carbonyl oxygen donor atoms in a *trans* geometry. The previously reported lake pigments of this type result in 1-dimensional coordination polymers formed as the sulfonate group bridges two metal ions to give an eight-membered $[MOSOMOSO]_n$ (M = group 2 metal ion) repeat unit.[22] However, in this example, the steric hindrance of the morpholine unit obstructs further coordination of the sulfonate group and prevents the formation of a polymeric system. Arguably, the prevention of a polymeric species increases the solubility of the lake and allows the formation of larger crystals, as opposed to the microcrystalline powders that are often observed in similar systems. To the best of our knowledge, this is the first crystal structure of a pigment lake that has been isolated from DMSO,[21–24] and the nature of the solvent may also influence the aggregation of this species, because changes in solvent can change the aggregation of coordination polymers.

With a series of new dyes **6a**–**e** and **8** and pigments **15a**,**b**,**c** synthesized, their colour properties were next evaluated and compared with those of the morpholine-free reference compounds **9a**, **9b**, **10** and **16**. The absorption spectra of series **6** and **9** in $CHCl_3$ solution were recorded and are presented in Figure 7 and Table 3. The absorption bands of the new dyes **6** appear as single maxima in the range 475–491 nm, whereas the maxima for reference dyes **9a** and **9b** appear as broadened bands suggestive of two overlapping bands with maxima at 482 and 489 nm, respectively. Such broadening of the absorption bands of **9a** and **9b** renders comparison of the absorption-band full-width at half-maximum intensity with those of **6a**–**e** of little value. On comparison of the spectrum of **6a** with that of **9a**, it is clear that the morpholine unit induces a small hypsochromic shift in λ_{max} of 7 nm but with a significant hyperchromic effect, that is, the extinction coefficient for **6a** is ca. 1.5 times that of **9a**; this constitutes a beneficial feature. A similar comparison between the absorption data for the nitro-substituted dye **6e** and the reference compound **9b** revealed that the morpholine group again induced a small hypsochromic shift in λ_{max} of 9 nm, and the extinction coefficient of **6e** is 1.9 times larger than that of **9b**. The small hypsochromic shift induced by the morpholine residue may be rationalized by the limited additional electron donation from the morpholine unit, which is rather twisted relative to the naphthalene ring plane owing to the *peri* interaction between the $N(CH_2)_2$ unit and 5-H (Figure 5).

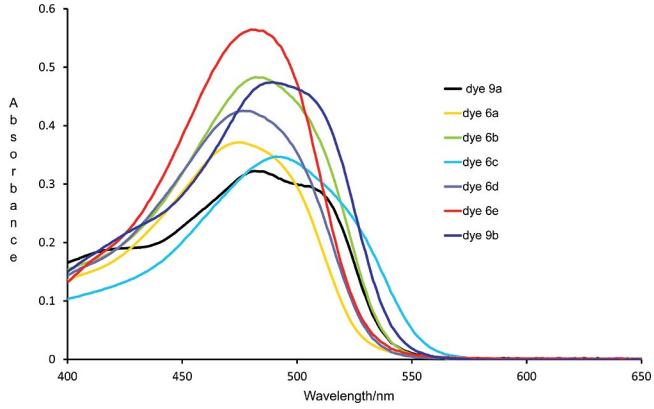

Figure 7. Absorption spectra ($CHCl_3$ solution) of dyes **6** and reference dye **9**.

Table 3. Spectroscopic data for dyes **6**, **8**, **9** and **10**.

Compound	λ_{max} ($CHCl_3$) [nm]	ε_{max} [$mol^{-1}\,dm^3cm^{-1}$]
6a	475	26250
6b	482	35100
6c	491	25650
6d	476	31200
6e	480	45650
9a	482	17400
9b	489	23950
8[a]	466	36950
10[a]	481	16500

[a] Data recorded in DMSO.

The optical spectra of the structures represented in Schemes 2 and 3 have been analyzed by first-principle methods, and the main theoretical results are summarized in Table 4. Firstly, it should be noted that, consistent with experimental IR and ^{13}C NMR spectroscopic and X-ray crystallographic data, the tautomeric equilibrium is systematically in favour of the hydrazone form. Indeed, the azo tautomer is by 1.5–3.8 kcal mol^{-1} less stable depending on the substituents. In addition, the equilibrium is more displaced for the nitro-substituted structures, which also fits the experimental findings. Consequently, only the computed spectroscopic results obtained with the hydrazone structures are discussed. As expected from the results from earlier investi-

gations of azobenzenes,[32] the computed λ_{max} values are smaller than those determined experimentally. However, the auxochromic effects are well predicted by time-dependent DFT (TD-DFT). Indeed, starting from **9a**, the addition of a nitro group induces a measured +7 nm (computed +10 nm) bathochromic displacement, whereas the morpholine group has the opposite effect and induces a displacement of –7 nm (–7 nm); the simultaneous addition of both groups leads to an insignificant impact on λ_{max}. Likewise, the inclusion of the morpholine group systematically induces a significant increase of the oscillator strength, which is consistent with the larger ε_{max} obtained experimentally (Table 3).

Table 4. Parameters computed by DFT and TD-DFT. ΔG is the relative stability of the hydrazone form (compared to the azo form), λ_{max} is the vertical transition wavelength, f is the corresponding oscillator strength (computed in SS-PCM, LR-PCM data in parentheses), q_{CT} and d_{CT} are the computed charge-transfer charge and distance, respectively.

Compound	ΔG [kcal/mol]	λ_{max} [nm]	f [au]	q_{CT} [e]	d_{CT} [Å]
9a	–1.57	401 (*412*)	0.53 (*0.64*)	0.46	1.21
6a	–2.76	394 (*404*)	0.73 (*0.87*)	0.50	1.40
9b	–2.41	411 (*419*)	0.68 (*0.82*)	0.49	0.68
6e	–3.75	404 (*412*)	0.99 (*1.16*)	0.53	0.47
10	–2.16	394 (*402*)	0.40 (*0.57*)	0.49	1.14
8	–2.80	385 (*393*)	0.61 (*0.81*)	0.52	1.27

The density difference plots shown in Figure 8 allow the qualitative understanding of the small variations of the absorption wavelengths induced by the nitro and morpholine groups. For **9a**, one notices that, though the excitation is highly delocalized, there is a small charge transfer (CT) from the two phenyl rings (mostly in blue) to the keto group (in red). In the dipolar approximation, this CT corresponds to the transfer of ca. 0.5 e over 1.2 Å (see Table 4). In **9b**, the addition of the nitro group allows extension of the conjugated path but at the price of a smaller CT (0.7 Å); these opposite effects explain why the obtained bathochromic shift is rather small. For **6e**, one clearly notices that the expected push–pull effect is very limited: There is no clear-cut electron transfer from the morpholine ring to the nitro group but rather a fully delocalized π–π* transition. The estimated CT distance is actually the smallest of the series (0.5 Å).

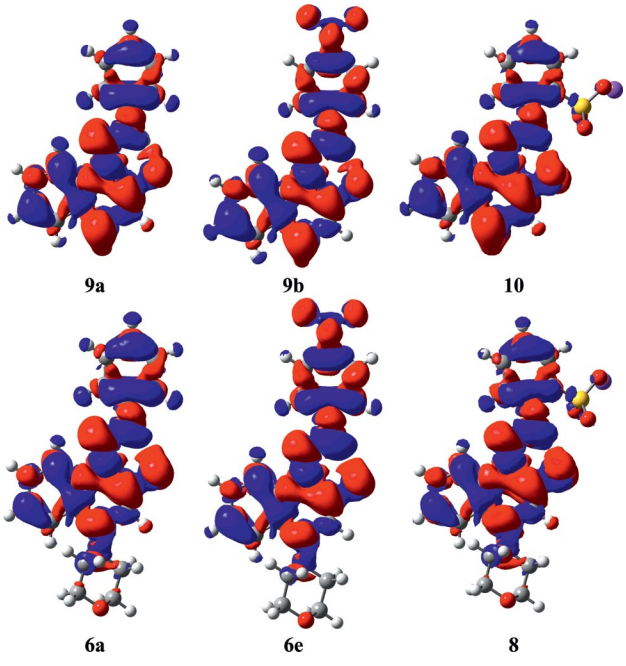

Figure 8. Density difference plots for the six dyes investigated. The blue (red) regions indicate decrease (increase) of the electron density upon photon absorption.

The absorption spectra of **8** and **10** are presented in Figure 9. On comparison of the spectra of **8** and **10**, it is evident once again that the morpholine unit induces a hypsochromic shift in λ_{max} of 15 nm accompanied by significant hyperchromism; the extinction coefficient for **8** is ca. 2.2 times that of **10**, and these data are again nicely predicted by theory (see Table 4). It is acknowledged that changes in dye structure do result in modification of molar extinction coefficients. However, for some representative azo dyes these changes are typically up to a maximum of ±20% of the value of the reference compound,[33] whereas in the current study the extinction coefficients increase in the range 50–120% upon inclusion of the morpholine unit.

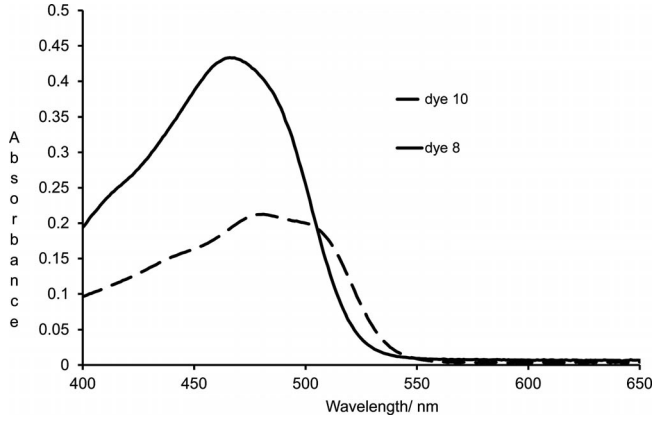

Figure 9. Absorption spectra (DMSO solution) of dyes **8** and reference dye **10**.

The evaluation of the colour of the pigment lakes **15** and **16** was accomplished by reflectance measurements of a polyurethane film containing the pigment sandwiched between two microscope slides. The Commission Internationale de l'Éclairage (CIE) $L^*a^*b^*$[34] colour coordinates are presented in Table 5. These data reveal broadly comparable a^* values; significant variations in the b^* values lead to pigments **15**, **15a** and **15b** appearing orange owing to the larger

Table 5. CIE $L^*a^*b^*$ colour coordinates for pigment lakes **15** and **16**.

Compound	L^*	a^*	b^*
15	49.55	42.93	39.36
15a	49.85	45.07	42.48
15b	53.77	44.17	46.30
15c	33.76	25.06	14.41
16	39.80	43.59	25.23

*b** (yellow) contribution, whereas **16**, which has a significantly decreased *b** contribution, appears red. Pigment lake **15c**, derived from **15a**, was the least bright, most red sample in accord with the observation that **15a** darkened as it was heated under vacuum.

Notably, in comparison to the wealth of red and yellow lake pigments,[10] there are relatively few available orange pigment lakes derived from substituted 2-napthols, for example, the barium lake Pigment Orange 17 and the aluminium analogue, Pigment Orange 17:1; this new pigment lake **15** may be a useful addition to the armoury of the colourist.

Conclusions

The presence of the morpholine substituent at C-4 in a new series of ketohydrazone dyes derived from 4-morpholino-2-naphthol and a series of anilines results in enhanced molar extinction coefficients relative to those of their morpholine-free counterparts. The increased molar extinction coefficients are consistent with increased oscillator strengths ascertained by TD-DFT computations. The crystal structure of a new pigment lake DMSO solvate is described. In the solid state, the steric bulk of the morpholine substituent obstructs further coordination of the bridging sulfonate groups and prevents the formation of a 1-dimensional polymeric system involving the eight-membered repeating unit that has been proposed for other pigment lakes. The colour enhancement combined with the relative ease of crystallization may render such pigments, with a hitherto unexplored substitution pattern, useful as new colourants.

Experimental Section

Equipment and Reagents: Unless otherwise stated, reagents were used as supplied by major chemical suppliers. 4-Morpholino-2-naphthol was provided by Vivimed Laboratories (Europe) Ltd., Leeds Road, Huddersfield. Para Red [1-(4-nitrophenylazo)-2-naphthol] **9b** was purchased from Acros Organics and crystallized before use. NMR spectra were recorded with a Bruker Avance 400 MHz spectrophotometer (^{1}H NMR 400 MHz, ^{13}C NMR 100 MHz) for sample solutions in $CDCl_3$ with tetramethylsilane as an internal reference unless stated otherwise. FTIR spectra were recorded with a Nicolet 38 FTIR spectrometer equipped with a diamond attenuated total reflectance (ATR) attachment (neat sample). The powder X-ray diffraction patterns were recorded with a Bruker D2 Phaser instrument operating in reflection mode [Cu-K_α radiation (1.5418 Å), step size 0.02°, angular range $5 < 2\theta < 50°$ over a period of 3 h]. The single-crystal X-ray diffraction data were collected with a Bruker Apex Duo diffractometer.[29] Scanning electron microscopy was performed with a Jeol JSM-6060LV instrument; samples were coated with Au(80%)/Pd(20%) prior to analysis. Thermogravimetric analyses were performed with a Mettler-Toledo TG50 Thermobalance with a TC15-TA controller over the range 25–450 °C at a heating rate of 10 °C min^{-1} under a flow (10 mL min^{-1}) of N_2. UV/Vis spectra were recorded for solutions of the samples in either spectroscopic-grade $CHCl_3$, EtOH or DMSO [10 mm pathlength quartz cuvette, poly(tetrafluoroethylene) (PTFE) capped, concentration range ca. 1×10^{-4}–10^{-6} mol dm^{-3}] with an Agilent (Cary) 60 spectrophotometer. The reflectance spectra of pigment lakes were measured in a polyurethane film (10% pigment to polyurethane w/w), sandwiched between microscope slides against a white card background by using a Minolta spectrophotometer model CM-3700d (Xe flash simulating natural daylight, D65, diffuse illumination, collected at 10° to normal). All new dyes were homogeneous by TLC with a range of eluent systems of differing polarity. Mass spectra [Thermo (Finnigan) LTQ OrbitrapXL] were recorded at the National EPSRC Mass Spectrometry Service Centre, Swansea.

TD-DFT Calculations: For general azobenzene dyes, a benchmark investigation was performed previously,[32] and the recommended method has been applied. All quantum mechanical simulations have been performed with the Gaussian 09 program.[35] The CAM-B3LYP exchange-correlation functional was selected for all calculations,[36] which provided consistent estimates of the auxochromic shifts, though the absorption wavelengths are typically underestimated. First geometry optimizations in both chloroform and DMSO have been performed by using the C-PCM (conducting polarizable continuum model) solvent model[37] and the 6-311G(d,p) atomic basis set. In the second step, vibrational calculations were used to establish that the optimized structures corresponded to true minima of the potential energy surface. In the third stage, the first five lowest-lying singlet excited states were determined within the vertical C-PCM-TD-DFT approximation by using the 6-311+G(d,p) atomic basis set. The latter calculations were performed with the state-specific nonequilibrium PCM (SS-PCM) approach,[38] though the differences with the standard linear-response PCM approach were negligible for the considered dyes. For the first strongly dipole-allowed states, we determined the difference of electronic density between ground and excited states with LR-PCM-TD-DFT, which allows chemically sound representations of the impact of the electronic transitions implying a complex orbital blend. A threshold of 0.0004 au (atomic units) has been used to plot these density differences. A recently developed approach to estimate the charge transfer has been applied to further characterize the excited states.[39,40]

General Method for the Preparation of Dyes Derived from a 2-Naphthol and an Aniline: A freshly prepared cold (ca. 5 °C) solution of sodium nitrite (55 mmol) in water (25 mL) was added portionwise to a cold (ca. 5 °C), stirred solution of aniline (50 mmol) in aqueous HCl (50% v/v, 32 mL) at such a rate so as to maintain the temperature below ca. 10 °C. Upon completion of the addition, the cold solution was stirred for 15 min. The cold solution of the diazonium salt was slowly added to a cold stirred solution/suspension of a 2-naphthol (50 mmol) in aqueous NaOH (10% w/v, 50 mL). The resulting cold intense red-orange suspension was stirred for 1 h. The precipitated crude product was collected by vacuum filtration and washed well with water and then air-dried. The pure compounds were obtained by crystallization from a minimum volume of glacial acetic acid, washed with a minimum volume of ice-cold ethanol and subsequently dried overnight at 70 °C. The following compounds were prepared by this general protocol.

(*Z*)-1-(2-Phenylhydrazono)-4-morpholinonaphthalen-2(1*H*)-one (6a): Bright orange microneedles, 11.5 g (69%), m.p. 203–205 °C. UV/Vis ($CHCl_3$): λ_{max} (ε_{max}, mol^{-1} dm^3 cm^{-1}) = 475 (26250) nm. UV/Vis (MeOH): λ_{max} (ε_{max}, mol^{-1} dm^3 cm^{-1}) = 472 (24700) nm. FTIR: $\tilde{\nu}_{max}$ = 2977, 2838, 1595, 1584, 1489, 1371, 1248, 1202, 1113, 1020, 893, 725, 682, 430 cm^{-1}. ^{1}H NMR (400 MHz, $CDCl_3$): δ = 3.28 [t, J = 4.7 Hz, 4 H, $N(CH_2)_2$], 3.99 [t, J = 4.7 Hz, 4 H, $O(CH_2)_2$], 6.28 (s, 1 H, 3-H), 7.20 (m, 1 H, Ar-H), 7.39 (m, 1 H, Ar-H), 7.45 (m, 2 H, Ar-H), 7.54 (m, 1 H, Ar-H), 7.61 (m, 2 H, Ar-H), 7.76 (dd, J = 8.1, 0.9 Hz, 1 H, 5-H), 8.49 (dd, J = 8.2, 1.0 Hz, 1 H, 8-H), 16.24

(br. s, 1 H, NH) ppm. ^{13}C NMR (100 MHz, $CDCl_3$): δ = 52.4, 66.7, 111.6, 116.6, 122.9, 124.7, 125.1, 125.3, 125.7, 128.9, 129.2, 129.6, 134.8, 142.9, 161.2, 178.7 ppm. HRMS: calcd. for $C_{20}H_{19}N_3O_2$ $[M + H]^+$ 334.1550; found 334.1554.

(*Z*)-1-[2-(4-Methylphenyl)hydrazono]-4-morpholinonaphthalen-2(1*H*)-one (6b): Bright orange microneedles, 10.4 g (60%), m.p. 197–199 °C. UV/Vis ($CHCl_3$): λ_{max} (ε_{max}, $mol^{-1}\,dm^3\,cm^{-1}$) = 482 (35100) nm. FTIR $\tilde{\nu}_{max}$ = 2974, 2836, 1597, 1584, 1489, 1365, 1251, 1113, 884, 764, 506, 433 cm^{-1}. ^{1}H NMR (400 MHz, $CDCl_3$): δ = 2.40 (s, 3 H, Me), 3.26 [t, J = 4.7 Hz, 4 H, $N(CH_2)_2$], 3.98 [t, J = 4.7 Hz, 4 H, $O(CH_2)_2$], 6.27 (s, 1 H, 3-H), 7.24 (m, 2 H, Ar-H), 7.37 (m, 1 H, Ar-H), 7.53 (m, 3 H, Ar-H), 7.77 (dd, J = 8.1, 0.9 Hz, 1 H, 5-H), 8.49 (dd, J = 8.2, 1.0 Hz, 1 H, 8-H), 16.35 (br. s, 1 H, NH) ppm. ^{13}C NMR (100 MHz, $CDCl_3$): δ = 21.1, 52.4, 66.8, 111.7, 116.8, 122.7, 124.5, 124.9, 125.4, 128.5, 129.0, 130.1, 134.8, 135.5, 140.8, 160.7, 177.8 ppm. HRMS: calcd. for $C_{21}H_{21}N_3O_2$ $[M + H]^+$ 348.1707; found 348.1710.

(*Z*)-1-[2-(4-Methoxylphenyl)hydrazono]-4-morpholinonaphthalen-2(1*H*)-one (6c): Bright orange microneedles, 11.7 g (64%), m.p. 180–182 °C. UV/Vis ($CHCl_3$): λ_{max} (ε_{max}, $mol^{-1}\,dm^3\,cm^{-1}$) = 491 (25650) nm. FTIR: $\tilde{\nu}_{max}$ = 2967, 2830, 1606, 1584, 1555, 1493, 1371, 1241, 1203, 1177, 1113, 1021, 894, 827, 765, 728, 520, 434 cm^{-1}. ^{1}H NMR (400 MHz, $CDCl_3$): δ = 3.27 [t, J = 4.7 Hz, 4 H, $N(CH_2)_2$], 3.88 (s, 3 H, OMe), 3.99 [t, J = 4.7 Hz, 4 H, $O(CH_2)_2$], 6.38 (s, 1 H, 3-H), 7.00 (m, 2 H, Ar-H), 7.38 (m, 1 H, Ar-H), 7.54 (m, 1 H, Ar-H), 7.62 (m, 2 H, Ar-H), 7.81 (dd, J = 8.2, 0.7 Hz, 1 H, 5-H), 8.53 (dd, 1 H, J = 8.1, 0.8 Hz, 8-H), 16.40 (br. s, 1 H, NH) ppm. ^{13}C NMR (100 MHz, $CDCl_3$): δ = 52.5, 55.6, 66.8, 111.1, 114.9, 118.8, 122.5, 124.2, 124.8, 125.1, 128.1, 128.8, 134.8, 137.7, 158.3, 159.9, 174.5 ppm. HRMS: calcd. for $C_{21}H_{21}N_3O_3$ $[M + H]^+$ 364.1656; found 364.1658.

(*Z*)-1-[2-(4-Chlorophenyl)hydrazono]-4-morpholinonaphthalen-2(1*H*)-one (6d): Bright orange microneedles, 12.5 g (68%), m.p. 226–228 °C. UV/Vis ($CHCl_3$): λ_{max} (ε_{max}, $mol^{-1}\,dm^3\,cm^{-1}$) = 476 (31200) nm. FTIR: $\tilde{\nu}_{max}$ = 2974, 2835, 1592, 1581, 1487, 1386, 1364, 1251, 1216, 1202, 1112, 882, 765, 733, 504, 426, 418 cm^{-1}. ^{1}H NMR (400 MHz, $CDCl_3$): δ = 3.27 [t, J = 4.7 Hz, 4 H, $N(CH_2)_2$], 3.98 [t, J = 4.7 Hz, 4 H, $O(CH_2)_2$], 6.23 (s, 1 H, 3-H), 7.40 (m, 3 H, Ar-H), 7.53 (m, 3 H, Ar-H), 7.54 (m, 1 H, Ar-H), 7.74 (dd, J = 8.1, 0.8 Hz, 1 H, Ar-H), 7.81 (dd, J = 8.2, 0.7 Hz, 1 H, 5-H), 8.45 (dd, J = 8.1, 0.8 Hz, 1 H, 8-H), 16.20 (br. s, 1 H, NH) ppm. ^{13}C NMR (400 MHz, $CDCl_3$): δ = 52.3, 66.7, 111.4, 117.6, 122.9, 124.8, 125.2, 125.9, 129.2, 129.3, 129.6, 130.2, 134.6, 141.7, 161.4, 178.8 ppm. HRMS: calcd. for $C_{20}H_{18}ClN_3O_2$ $[M + H]^+$ 368.1160; found 368.1165.

(*Z*)-1-[2-(4-Nitrophenyl)hydrazono]-4-morpholinonaphthalen-2(1*H*)-one (6e): 4-Nitroaniline (50 mmol) was dissolved in hot aqueous HCl (50% v/v, 32 mL), and the mixture was cooled rapidly to 0–5 °C to afford a fine suspension of 4-nitroaniline hydrochloride. A freshly prepared cold (ca. 5 °C) solution of sodium nitrite (60 mmol) in water (25 mL) was added portionwise to the cold (ca. 5 °C), stirred fine suspension of 4-nitroaniline (50 mmol) at such a rate so as to maintain the temperature below ca. 10 °C. The resulting cold solution of the diazonium salt was slowly added to a cold stirred suspension of 4-morpholino-2-naphthol (50 mmol) in aqueous NaOH (10% w/v, 50 mL). Upon completion of the addition, the resulting cold intense red-orange suspension was stirred for 1 h. The precipitated crude product was collected by vacuum filtration, washed well with water and then air-dried. Crystallization from a minimum volume of glacial acetic acid and washing with a minimum volume of ice-cold ethanol gave **6e** as a bright orange powder after drying at 70 °C overnight; 10.6 g (56%), m.p. 257–259 °C. UV/Vis ($CHCl_3$): λ_{max} (ε_{max}, $mol^{-1}\,dm^3\,cm^{-1}$) = 480 (45650) nm. FTIR: $\tilde{\nu}_{max}$ = 2854, 1590, 1566, 1498, 1388, 1368, 1324, 1220, 1105, 1024, 837, 776, 731, 418 cm^{-1}. ^{1}H NMR (400 MHz, $CDCl_3$): δ = 3.33 [t, J = 4.7 Hz, 4 H, $N(CH_2)_2$], 3.98 [t, J = 4.7 Hz, 4 H, $O(CH_2)_2$], 6.14 (s, 1 H, 3-H), 7.45 (m, 1 H, Ar-H), 7.56 (m, 3 H, Ar-H), 7.71 (d, J = 8.0 Hz, 1 H, 5-H), 8.27 (m, 2 H, Ar-H), 8.41 (d, J = 8.0 Hz, 1 H, 8-H), 16.00 (br. s, 1 H, NH) ppm. ^{13}C NMR: δ = 52.2, 66.5, 111.0, 115.4, 123.7, 125.6, 125.8, 127.2, 129.8, 131.4, 134.1, 143.4, 148.0, 162.7, 180.9 ppm. HRMS: calcd. for $C_{20}H_{18}N_4O_4$ $[M + H]^+$ 379.1401; found 379.1405.

General Method for the Preparation of Dyes Derived from a 2-Naphthol and Orthanilic Acid: A solution of sodium nitrite (60 mmol) in water (20 mL) was added in a single portion to a cool (ca. 10 °C) solution of orthanilic acid (55 mmol) and sodium carbonate (50 mmol) in water (100 mL). This solution was added slowly to a mixture of concentrated HCl (12 mL) and ice (50 g), and the mixture was maintained at ca. 5 °C. A cool suspension of the naphthol (50 mmol) in aqueous NaOH (10% w/v, 50 mL) was steadily added to the cool, stirred suspension of the diazotized orthanilic acid, and the resulting deep orange-red suspension/slurry was stirred for 30 min. The resulting paste was heated to ca. 70 °C, NaCl (25 g) was added, and the mixture stirred for 10 min and then cooled to ca. 5 °C in an ice bath. The crude product was collected by vacuum filtration and washed with a little cold water followed by a little EtOH and then Et_2O. The crude product was dissolved in a minimum volume of hot water, and the solution was then diluted with ethanol until crystallization/precipitation commenced. The pure product was collected from the cold solution by vacuum filtration and was washed with a little EtOH and finally with Et_2O. Samples were dried in an oven at 110 °C for 6 h. The following compound was obtained by this general procedure.

Sodium (*Z*)-2-{2-[4-Morpholino-2-oxonaphthalen-1(2*H*)-ylidene]-hydrazinyl}benzenesulfonate (8): Bright orange powder; 18.3 g (84%), m.p. 340 °C (dec.). UV/Vis (DMSO, D_2O): λ_{max} = 466 (36950) nm. FTIR: $\tilde{\nu}_{max}$ = 2952, 3835, 1573, 1494, 1480, 1240, 1190, 1019, 894, 710, 611, 425 cm^{-1}. ^{1}H NMR (400 MHz, D_2O, [D_6]DMSO): δ = 3.17 [t, J = 4.7 Hz, 4 H, $N(CH_2)_2$], 3.78 [t, J = 4.7 Hz, 4 H, $O(CH_2)_2$], 5.96 (s, 1 H, 3-H), 7.13 (m, 1 H, Ar-H), 7.31 (m, 1 H, Ar-H), 7.41 (m, 1 H, Ar-H), 7.49 (m, 1 H, Ar-H), 7.60 (m, 1 H, Ar-H), 7.67 (d, J = 7.1 Hz, 1 H, Ar-H), 7.98 (d, J = 8.2 Hz, 1 H, 5-H), 8.18 (d, J = 8.3 Hz, 1 H, 8-H) ppm. ^{1}H NMR (400 MHz, D_2O): δ_H = 3.11 [br. s, 4 H, $N(CH_2)_2$], 3.74 [br, s, 4 H, $O(CH_2)_2$], 5.80 (s, 1 H, 3-H), 7.09 (m, 1 H, Ar-H), 7.17 (m, 1 H, Ar-H), 7.29 (m, 1 H, Ar-H), 7.45 (m, 2 H, Ar-H), 7.67 (d, J = 7.8 Hz, 1 H, Ar-H), 7.85 (d, J = 8.3 Hz, 1 H, 5-H), 7.96 (d, J = 8.0 Hz, 1 H, 8-H) ppm. HRMS: calcd. for $C_{16}H_{11}N_2O_4S$ $[M - Na]^-$ 412.0973; found 412.0963.

General Method for the Preparation of Calcium Pigment Lakes Derived from (*Z*)-2-{2-[2-Oxonaphthalen-1(2*H*)-ylidene]hydrazinyl}-benzenesulfonates: A hot (80 °C) solution of $CaCl_2{\cdot}6H_2O$ (6 g) in water (40 mL) was added in a single portion to a vigorously stirred red-orange solution of a sodium (*Z*)-2-{2-[2-oxonaphthalen-1(2*H*)-ylidene]hydrazinyl}benzenesulfonate (5 g) in hot (80–90 °C) water (175 mL). The resulting voluminous precipitate was stirred at ca. 80 °C for 2 h and then cooled to 40 °C. The crude pigment lake was collected by filtration and washed well with water before air-drying and subsequent oven-drying at 110 °C overnight. A sample of each of the crude red-orange pigment lakes (1.50 g) was then purified by the following methods: (1) The pigment lake was dissolved in hot DMSO (ca. 15 mL) and precipitated by the addition of water. The precipitated pigment lake was collected by vacuum filtration, washed well with water and then dried at 120 °C. (2) The

pigment lake was crystallized from DMSO (ca. 15 mL); the crystallized pigment lake was collected by filtration, washed well with Et_2O and dried at 120 °C.

Calcium lake **15** derived from sodium (*Z*)-2-{2-[4-morpholino-2-oxonaphthalen-1(2*H*)-ylidene]hydrazinyl}benzenesulfonate (**8**) was obtained as an amorphous orange solid; crude yield 3.65 g. Conditioning: (1) crystallization of a 1.50 g sample from DMSO (**15a**); recovery 1.41 g (94%) as red-orange microneedles; m.p. 320 °C (dec.). FTIR: $\tilde{\nu}_{max}$ = 2952 (w), 2812 (w), 1591, 1574, 1492, 1446, 1390, 1371, 1252, 1206, 1174, 1111, 1077, 1016, 964, 894, 750, 706, 610, 596, 826, 445 cm^{-1}. ^1H NMR (400 MHz, [D_6]DMSO): δ = 2.54 [s, 6 H, $(CH_3)_2SO$ from solvate], 3.18 [br. m, 4 H, $N(CH_2)_2$], 3.86 [br. t, J = 3.8 Hz, 1 H, $O(CH_2)_2$], 6.05 (s, 1 H, 3-H), 7.13 (apparent t, 1 H, Ar-H), 7.44 (m, 2 H, Ar-H), 7.56 (apparent t, 1 H, Ar-H), 7.72 (dd, J = 7.7, 1.0 Hz, 1 H, Ar-H), 7.77 (d, J = 8.0 Hz, 1 H, Ar-H), 8.02 (d, J = 8.2 Hz, 1 H, 5-H), 8.38 (d, J = 7.9 Hz, 1 H, 8-H), 15.72 (s, 1 H, NH) ppm. ^{13}C NMR (100 MHz, [D_6]DMSO): δ = 40.9, 52.4, 66.4, 111.6, 116.4, 123.1, 123.8, 125.2, 126.0, 126.6, 127.9, 129.1, 129.7, 130.7, 134.9, 135.9, 140.1, 160.8, 178.3 ppm. (2) Precipitation of a 1.50 g sample from DMSO/H_2O (**15b**); recovery 1.38 g (92%) as an orange powder, m.p. 335 °C (dec.). FTIR: $\tilde{\nu}_{max}$ = 2848 (w), 1587, 1572, 1544, 1480, 1435, 1397, 1249, 1205, 1163, 1101, 1024, 996, 895, 753, 708, 615, 593, 514, 454 cm^{-1}. ^1H NMR (400 MHz, [D_6]DMSO): δ = 3.18 [br. m, 4 H, $N(CH_2)_2$], 3.85 [br. m, 1 H, $O(CH_2)_2$], 6.05 (s, 1 H, 3-H), 7.13 (apparent t, 1 H, Ar-H), 7.46 (m, 2 H, Ar-H), 7.56 (apparent t, 1 H, Ar-H), 7.74 (m, 2 H, Ar-H), 8.02 (d, J = 8.2 Hz, 1 H, 5-H), 8.37 (d, J = 8.0 Hz, 1 H, 8-H), 15.73 (s, 1 H, NH) ppm. ^{13}C NMR (100 MHz, [D_6]DMSO): δ = 52.4, 66.4, 111.6, 116.4, 123.1, 123.9, 125.2, 126.0, 126.6, 127.9, 129.2, 129.8, 130.8, 134.9, 135.8, 140.1, 160.9, 178.3 ppm.

Supporting Information (see footnote on the first page of this article): Additional experimental details, characterization data, and copies of the ^1H and ^{13}C NMR, IR, and mass spectra of key intermediates and final products.

Acknowledgments

The authors thank the Engineering and Physical Sciences Research Council (EPSRC) for access to the National Mass Spectrometry Service (Swansea), M. J. Scott (thermal analyses), Dr. H. Williams (SEM analysis) and Drs. S. M. Partington, S. N. Corns and A. Towns at Vivimed Laboratories (Europe). D. J. acknowledges the European Research Council (ERC) and the Région des Pays de la Loire for financial support in the framework of a Starting Grant (Marches – 278845) and a Recrutement sur Poste Stratégique, respectively. This research used resources of the Grand Equipement National de Calcul Intensif-Centre Informatique National de l'Enseignement Supérieur/Institut de Développement et des Ressources en Informatique Scientifique (GENCI-CINES/IDRIS), the Centre de Calcul Intensif des Pays de Loire (CCIPL) and a local Troy cluster (Université de Nantes).

[1] M. Rickwood, K. E. Smith, C. D. Gabbutt, J. D. Hepworth, PCT WO 94/22850, **1994**.
[2] B. Van Gemert, D. B. Knowles, US Patent, US 5,552,090, **1996**.
[3] D. A. Clarke, B. M. Heron, C. D. Gabbutt, J. D. Hepworth, S. M. Partington, S. N. Corns, PCT WO 98/45281, **1998**.
[4] O. Breyne, Y.-P. Chan, D. Henry, X. Lafosse, PCT WO 98/50807, **1998**.
[5] J. Momoda, S. Matsuoka, H. Nagou, US 6525194 B1, **2003**.
[6] G. M. Iskander, S. A. Sarrag, S. Stansfield, *J. Chem. Soc. C* **1971**, 1701–1703.
[7] A. V. Didenko, V. V. Labeish, A. V. Trukhin, M. L. Petrov, *Russ. J. Org. Chem. (Engl. Transl.)* **2007**, *43*, 1092–1095.
[8] S. C. Benson, J. Y. L. Lam, K. G. Upadhya, P. A. Radel, W. Zhen, S. M. Menchen, US 6051719, **2000**.
[9] K. Hunger (Ed.), *Industrial Dyes: Chemistry, Properties, Applications*, Wiley-VCH, Weinheim, **2003**.
[10] W. Herbst, K. Hunger (Eds.), *Industrial Organic Pigments: Production, Properties, Application*, Wiley-VCH, Weinheim, **1993**.
[11] Standard texts for diazotization and coupling include: a) A. I. Vogel, B. S. Furniss, A. J. Hannaford, V. Rogers, P. W. G. Smith, A. R. Tatchell, *Vogel's Textbook of Practical Organic Chemistry*, 4th ed., Longman, New York, **1978**, pp. 687–721; b) K. H. Saunders, R. L. M. Allen in *Aromatic Diazo Compounds*, 3rd ed., Edward Arnold Publishers Ltd., London, **1985**; c) K. Venkataraman, *The Chemistry of Synthetic Dyes*, Academic Press, New York, **1952**, vol. 1, pp. 210–240; d) J. M. Tedder in *The Chemistry of Synthetic Dyes*, vol. 3 (Ed.: K. Venkataraman), Academic Press, New York, **1970**, pp. 223–248; e) C. V. Stead in *The Chemistry of Synthetic Dyes*, vol. 3 (Ed.: K. Venkataraman), Academic Press, New York, **1970**, pp. 249–301; f) H. Zollinger, *Colour Chemistry*, 2nd ed., VCH Publishers, Weinheim, **1991**, pp. 109–186.
[12] a) A. Lyčka, *Ann. Rep. NMR Spectrosc.* **1993**, *26*, 247–281; b) A. Lyčka, J. Jirman, M. Nečas, *Dyes Pigm.* **1991**, *15*, 23–29.
[13] G. Pavlović, L. Racané, H. Čičak, V. Tralić-Kulenović, *Dyes Pigm.* **2009**, *83*, 354–362.
[14] P. Gilli, V. Bertolasi, L. Pretto, L. Antonov, G. Gilli, *J. Am. Chem. Soc.* **2005**, *127*, 4943–4953.
[15] A. C. Olivieri, R. B. Wilson, I. C. Paul, D. Y. Curtin, *J. Am. Chem. Soc.* **1989**, *111*, 5525–5532.
[16] S. H. Alarcón, A. C. Olivieri, D. Sanz, R. M. Claramunt, J. Elguero, *J. Mol. Struct.* **2004**, *705*, 1–9.
[17] S. H. Alarcón, A. C. Olivieri, P. Jonsen, *J. Chem. Soc. Perkin Trans. 2* **1993**, 1783–1786.
[18] a) W. M. F. Fabian, L. Antonov, D. Nedeltcheva, F. S. Kamounah, P. J. Taylor, *J. Phys. Chem. A* **2004**, *108*, 7603–7612; b) T. Hihara, Y. Okada, Z. Morita, *Dyes Pigm.* **2003**, *59*, 25–41.
[19] a) A. Lyčka, *Dyes Pigm.* **1999**, *43*, 27–32; b) A. Lyčka, D. Šnobl, V. Macháček, M. Večeřa, *Org. Magn. Reson.* **1981**, *16*, 17–19.
[20] a) R. M. Christie, J. L. Mackay, *Color. Technol.* **2008**, *124*, 133–144; b) J. Lenoir in *The Chemistry of Synthetic Dyes*, vol. 5 (Ed.: K. Venkataraman), Academic Press, New York, **1971**, pp. 313–474.
[21] A. R. Kennedy, C. McNair, W. E. Smith, G. Chisholm, S. J. Teat, *Angew. Chem.* **2000**, *112*, 652; *Angew. Chem. Int. Ed.* **2000**, *39*, 638–640.
[22] A. R. Kennedy, H. Stewart, K. Eremin, J. Stenger, *Chem. Eur. J.* **2012**, *18*, 3064–3069.
[23] S. L. Bekö, S. M. Hammer, M. U. Schmidt, *Angew. Chem.* **2012**, *124*, 4814; *Angew. Chem. Int. Ed.* **2012**, *51*, 4735–4738.
[24] T. Gorelik, M. U. Schmidt, J. Brüning, S. L. Bekö, U. Kolb, *Cryst. Growth Des.* **2009**, *9*, 3898–3903.
[25] a) M. U. Schmidt, US 6228162 B1, **2001**; b) F. Schui, R. Deubel, N. Wester, US 4719292, **1988**; c) P. Erk, *Curr. Opin. Solid State Mater. Sci.* **2001**, *5*, 155–160.
[26] S. N. Ivashevskaya, J. van de Streek, J. E. Djanhan, J. Brüning, E. Alig, M. Bolte, M. U. Schmidt, P. Blaschka, H. W. Höffken, P. Erk, *Acta Crystallogr., Sect. B* **2009**, *65*, 212–222.
[27] C. F. Macrae, P. R. Edgington, P. McCabe, E. Pidcock, G. P. Shields, R. Taylor, M. Towler, J. van de Streek, *J. Appl. Crystallogr.* **2006**, *39*, 453–457.
[28] a) Z. Hao, A. Iqbal, *Chem. Soc. Rev.* **1997**, *26*, 203–213; b) K. Hunger, *Rev. Prog. Coloration* **1999**, *29*, 71–84.
[29] The single-crystal X-ray diffraction data were collected with a Bruker Apex Duo diffractometer equipped with a graphite-monochromated Mo-K_α radiation source and a cold stream of N_2 gas. Selected crystal data for **15a**: $C_{44}H_{48}CaN_6O_{12}S_4$, M = 1021.20, triclinic, a = 7.9827(3) Å, b = 10.8066(4) Å, c = 13.5195(5) Å, α = 87.416(1)°, β = 85.081(1)°, γ = 82.085(1)°, V

= 1150.25(7) Å^3, T = 150 K, space group $P1$, Z = 1, μ = 0.39 mm^{-1}, 30281 measured reflections, 7634 independent reflections (R_{int} = 0.018). The final R_1 value was 0.0318 [$I > 2\sigma(I)$]. The final $wR(F^2)$ value was 0.0882 [$I > 2\sigma(I)$]. The final R_1 value was 0.0378 (all data). The final $wR(F^2)$ value was 0.0927 (all data). The goodness of fit on F^2 was 1.039. Largest peak/hole 0.44/–0.43 e Å^{-3}. CCDC-945706 contains the supplementary crystallographic data for this paper. These data can be obtained free of charge from The Cambridge Crystallographic Data Centre via www.ccdc.cam.ac.uk/data_request/cif.

[30] C. Astbury, L. K. Conway, C. Gillespie, K. Hodge, E. Innes, A. R. Kennedy, *Dyes Pigm.* **2013**, *97*, 100–104.

[31] L. Racané, Z. Mihalić, H. Cerić, J. Popović, V. Tralić-Kulenović, *Dyes Pigm.* **2013**, *96*, 672–678.

[32] D. Jacquemin, J. Preat, E. A. Perpète, D. P. Vercauteren, J. M. André, I. Ciofini, C. Adamo, *Int. J. Quantum Chem.* **2011**, *111*, 4224–4240.

[33] a) J. Griffiths, B. Roozpeilar, *J. Chem. Soc. Perkin Trans. 1* **1976**, 42–45; b) E. Sawiki, *J. Org. Chem.* **1957**, *22*, 915–919.

[34] *C. I. E. Technical, Report: Colorimetry*, 3rd ed., Commission Internationale de l'Eclairage, (Editorial Committee: E. C. Carter, Y. Ohno, M. R. Pointer, AR. Robertson, R. Seve, J. D. Schanda, K. Witt), Vienna, Austria, **2004**.

[35] M. J. Frisch, G. W. Trucks, H. B. Schlegel, G. E. Scuseria, M. A. Robb, J. R. Cheeseman, G. Scalmani, V. Barone, B. Mennucci, G. A. Petersson, H. Nakatsuji, M. Caricato, X. Li, H. P. Hratchian, A. F. Izmaylov, J. Bloino, G. Zheng, J. L. Sonnenberg, M. Hada, M. Ehara, K. Toyota, R. Fukuda, J. Hasegawa, M. Ishida, T. Nakajima, Y. Honda, O. Kitao, H. Nakai, T. Vreven, J. A. Montgomery, J. E. Peralta, F. Ogliaro, M. Bearpark, J. J. Heyd, E. Brothers, K. N. Kudin, V. N. Staroverov, R. Kobayashi, J. Normand, K. Raghavachari, A. Rendell, J. C. Burant, S. S. Iyengar, J. Tomasi, M. Cossi, N. Rega, J. M. Millam, M. Klene, J. E. Knox, J. B. Cross, V. Bakken, C. Adamo, J. Jaramillo, R. Gomperts, R. E. Stratmann, O. Yazyev, A. J. Austin, R. Cammi, C. Pomelli, J. W. Ochterski, R. L. Martin, K. Morokuma, V. G. Zakrzewski, G. A. Voth, P. Salvador, J. J. Dannenberg, S. Dapprich, A. D. Daniels, Ö. Farkas, J. B. Foresman, J. V. Ortiz, J. Cioslowski, D. J. Fox, *Gaussian 09*, Revision C.01, Gaussian Inc., Wallingford, CT, **2009**.

[36] T. Yanai, D. P. Tew, N. C. Handy, *Chem. Phys. Lett.* **2004**, *393*, 51–56.

[37] J. Tomasi, B. Mennucci, R. Cammi, *Chem. Rev.* **2005**, *105*, 2999–3094.

[38] R. Improta, V. Barone, G. Scalmani, M. J. Frisch, *J. Chem. Phys.* **2006**, *125*, 054103.

[39] T. Le Bahers, C. Adamo, I. Ciofini, *J. Chem. Theory Comput.* **2011**, *7*, 2498–2506.

[40] D. Jacquemin, T. Le Bahers, C. Adamo, I. Ciofini, *Phys. Chem. Chem. Phys.* **2012**, *14*, 5383–5388.

Received: August 12, 2013
Published Online: October 31, 2013

